Molecular Motions of Supercoiled and Circular DNA. A Phosphorus-31 Nuclear Magnetic Resonance Study

Peter Bendel,[†,§] Orgad Laub,[‡] and Thomas L. James*[†]

Contribution from the School of Pharmacy, Department of Pharmaceutical Chemistry, and School of Medicine, Department of Biochemistry and Biophysics, University of California, San Francisco, San Francisco, California 94143. *Received February 17, 1982*

Abstract: We present the results of the first nuclear magnetic resonance (NMR) experiments on intact plasmid DNA in closed duplex, supercoiled form, in solution. The observed species was pIns36 (7200 base pairs long), which was derived from plasmid pBR322 containing a 2800 base pair DNA fragment (human insulin gene) subcloned into the *Hin*dIII site of pBR322. This DNA form proved suitable for growth and amplification in *Escherischia coli* strain HB101 at yields that produced the large quantities needed in NMR experiments. Measurements of the ^{31}P NMR spin-lattice relaxation time T_1, spin-spin relaxation time T_2, and $^{31}P\{^1H\}$ nuclear Overhauser effect (NOE) were conducted on the supercoiled, nicked-circular, and linear forms of pIns36 in solutions containing 0.1 M NaCl, 10 mM cacodylic acid, and 2 mM EDTA at pH 7.0 and 25 °C. The results for the linear form conform to previously published relaxation parameters on shorter DNA fragments: the relatively short spin-lattice relaxation times of 2.4 s and NOE values of 1.3 indicate the presence of a fast, subnanosecond internal motion, when relaxation times and NOE's are simulated by including contributions from both heteronuclear dipole-dipole and chemical shift anisotropy relaxation mechanisms. The spin-spin relaxation time value of 19 ms makes it necessary to invoke an additional slower, isotropic motion with a correlation time of 0.86 μs. The T_1 and NOE values in the nicked-circular and supercoiled forms are compatible with about the same correlation times for the internal motion as the linear DNA. The observed spin-spin relaxation times, however, are significantly different from the linear form, being 0.25 s in circular and 1.17 s in the supercoiled DNA. When analyzed with the same model for relaxation, these T_2 values lead to values of 56 and 5 ns, respectively, for the correlation time of the slower, isotropic motion. These changes in the isotropic reorientation times are much too large to be accounted for by considering the overall tumbling of the molecules (although the trend of these results is predicted by the decrease in the radius of gyration from the linear, through the circular, to the supercoiled form). This is further evidence for the notion that the isotropic reorientation effective in the ^{31}P NMR relaxation is caused by bending motions of the chain for molecules longer than one persistence length. It is suggested that the increased effective frequency of these bending motions observed for the closed DNA forms results mainly from an excess of conformational free energy and coupling to higher frequency torsional motions.

The flexibility and molecular dynamics of nucleic acids and polynucleotides in solution have been subject to numerous recent investigations by nuclear magnetic resonance.[1] So far, all the experiments have been carried out on linear and open-end DNA or polynucleotide molecules of variable chain lengths. It has been speculated that the dynamic properties of DNA, and not just its static structure, are significant in the understanding of how the DNA molecule performs its various biological functions. In this context, however, one cannot ignore the fact that a significant part of naturally occurring genetic material is in the form of covalently closed, or superhelical, DNA,[2,3] which exhibits some unique properties of chemical and biological reactivity.[3] Superhelicity has been found to be a requirement for a number of genetic processes, and enzymes that convert DNA between its topoisomers in vivo have been isolated and studied.[4,5]

We thus considered it worthwhile to employ ^{31}P NMR relaxation experiments to obtain information about the internal dynamics in superhelical DNA and compare it to the results obtained from the same DNA in its nicked-circular and linear forms. The structural constraints imposed on the double-helix axis by closing the molecule into a circle and by twisting it in superhelical turns introduce an excess of free energy into the molecule, compared to the linear form. It is therefore not unreasonable to expect that this excess free energy should manifest itself in different dynamical behavior for the various forms of DNA. It is already well-known that linear, circular, and supercoiled DNA of the same molecular weight exhibit different hydrodynamic properties such as sedimentation velocity and intrinsic viscosity. Furthermore, theoretical calculations show that the probability for base-pair opening sharply increases in supercoiled DNA.[6] On the other hand, no theoretical or experimental studies of internal and segmental motions in superhelical DNA have been reported, to the best of our knowledge.

[†] School of Pharmacy.
[‡] School of Medicine.
[§] Present address: Department of Isotope Research, Weizmann Institute of Science, Rehovot, Israel.

Theory

NMR Relaxation. The ^{31}P nucleus in nucleic acids relaxes mainly through heteronuclear dipole-dipole (DD) and chemical shift anisotropy (CSA) mechanisms. The selective dipole-dipole relaxation rates (obtained in the presence of proton decoupling) for ^{31}P coupled to a single hydrogen are given by[7] eq 1-3, where

$$(1/T_1)_{DD} = K[J_{DD}(\omega_H - \omega_P) + 3J_{DD}(\omega_P) + 6J_{DD}(\omega_H + \omega_P)] \quad (1)$$

$$(1/T_2)_{DD} = (1/2T_1)_{DD} + K[2J_{DD}(0) + 3J_{DD}(\omega_H)] \quad (2)$$

$$(NOE)_{DD} = 1 + \frac{\gamma_H}{\gamma_P} \frac{6J_{DD}(\omega_H + \omega_P) - J_{DD}(\omega_H - \omega_P)}{J_{DD}(\omega_H - \omega_P) + 3J_{DD}(\omega_P) + 6J_{DD}(\omega_H + \omega_P)} \quad (3)$$

T_1 and T_2 are the spin-lattice and spin-spin relaxation times, respectively, and NOE is the nuclear Overhauser enhancement of the signal intensity relative to the signal obtained without proton irradiation. γ_H and γ_P are the gyromagnetic ratios, and ω_H and ω_P are the Larmor frequencies of hydrogen and phosphorus. The $J(\omega)$ terms are the spectral densities of molecular motion, and the constant K is given by

$$K = (\hbar^2\gamma_P^2\gamma_H^2)/(20r^6) \quad (4)$$

where r is the proton-phosphorus internuclear distance.

(1) James, T. L. *Bull. Magn. Reson.*, in press (and references therein).
(2) Wang, J. C. *TIBS* **1980**, 219-221.
(3) Bauer, W. R. *Annu. Rev. Biophys. Bioeng.* **1978**, *7*, 287-313.
(4) Cozzaralli, N. R. *Science (Washington, D.C.)* **1980**, *207*, 953-960.
(5) Wang, J. C.; Liu, L. F. In "Molecular Genetics"; Academic Press: New York, 1979; pp 65-68.
(6) Vologodskii, A. V.; Lukoshin, A. V.; Anskelevich, V. V.; Frank-Kamenetskii, M. D. *Nucleic Acids Res.* **1979**, *6*, 967-982.
(7) Slichter, C. P. "Principles of Magnetic Resonance"; Harper and Row: New York, 1963.

0002-7863/82/1504-6748$01.25/0

In the case of CSA relaxation, the relevant equations are[8]

$$(1/T_1)_{CSA} = {}^6/_{40}\,\omega_P^2\delta_z^2(1 + (\eta^2/3))J_{CSA}(\omega_P) \quad (5)$$

and

$$(1/T_2)_{CSA} = {}^1/_{40}\,\omega_P^2\delta_z^2(1 + (\eta^2/3))[3J_{CSA}(\omega_P) + 4J_{CSA}(0)] \quad (6)$$

Here δ_z is the anisotropy and η the asymmetry of the chemical shift tensor. In the presence of both relaxation mechanisms, the combined relaxation rates are given by

$$1/T_{1,2} = (1/T_{1,2})_{DD} + (1/T_{1,2})_{CSA} \quad (7)$$

and

$$NOE = 1 + (NOE_{DD} - 1)(T_1/(T_1)_{DD}) \quad (8)$$

Analytical expressions for the spectral densities are based upon models for molecular motion. In the case of isotopic rotation characterized by a single correlation time τ_c, the spectral densities are

$$J_{DD}(\omega) = J_{CSA}(\omega) = (2\tau_c)/(1 + \omega^2\tau_c^2) \quad (9)$$

The assumption of a single isotropic motion is clearly an oversimplification for macromolecules such as DNA, and indeed, relaxation data for such molecules that consist of more than one measured parameter can rarely be fit to theory by assuming a single correlation time. Therefore, additional degrees of freedom with freely variable correlation times are usually introduced by means of various models. In these models a fast internal motion is usually superimposed on the slower, overall reorientation of the DNA molecule. For example, the overall reorientation can be approximated by the motion of a rigid ellipsoid about its short and long axes.[9] If the correlation times for this motion are considered fixed by the hydrodynamic properties of the linear DNA, the correlation time or jump rate of the internal motion remains as a variable for the fit to the experimental data. This approach seems to work reasonably well for relatively short DNA fragments (<300 base pairs).[10,11,35] For longer chains, the modeling of the whole molecule as a rigid rod becomes less realistic, and the use of Woessner's model[12] for free internal diffusion about an axis that itself undergoes isotropic reorientation has been proposed.[13-15] In this approach, both the overall and the internal motion correlation times are allowed to vary and the spectral densities for the dipolar interaction to be used in eq 1-3 are given by eq 10-15, where τ_0 and τ_i are the correlation times for the

$$J_{DD}(\omega) = A\frac{2\tau_0}{1 + \omega^2\tau_0^2} + B\frac{2\tau_B}{1+\omega^2\tau_B^2} + C\frac{2\tau_C}{1+\omega^2\tau_C^2} \quad (10)$$

$$A = {}^1/_4(3\cos^2\phi - 1)^2 \quad (11)$$

$$B = {}^3/_4\sin^2 2\phi \quad (12)$$

$$C = {}^3/_4\sin^4\phi \quad (13)$$

$$\tau_B = [1/\tau_0 + 1/(6\tau_i)]^{-1} \quad (14)$$

$$\tau_C = [1/\tau_0 + 2/(3\tau_i)]^{-1} \quad (15)$$

overall and internal motions, respectively, and ϕ is the angle between the phosphorus-hydrogen internuclear vector and the axis of internal rotation. The analogous equations for the spectral densities of the CSA mechanism, to be used in eq 5 and 6, were developed by Hull and Sykes:[16]

$$J_{CSA}(\omega) = \frac{1}{(1 + (\eta^2/3))}\sum_{j=0}^{2} C_j\frac{2\tau_j}{1 + \omega^2\tau_j^2} \quad (16)$$

Here τ_0, τ_1, and τ_2 are respectively identical with τ_0, τ_B, and τ_C in the dipolar case, and the geometrical coefficients are given in eq 17-19, where β and γ are the Euler angels rotating the

$$C_0 = {}^1/_4[(3\cos^2\beta - 1) + \eta\sin^2\beta\cos 2\gamma]^2 \quad (17)$$

$$C_1 = {}^1/_3\sin^2\beta[\cos^2\beta(3 - \eta\cos 2\gamma)^2 + \eta^2\sin^2 2\gamma] \quad (18)$$

$$C_2 = [(3/4)^{1/2}\sin^2\beta + (\eta/2(3^{1/2}))(1 + \cos^2\beta)\cos 2\gamma]^2 + (\eta^2/3)\sin^2 2\gamma\cos^2\beta \quad (19)$$

coordinate system of the internal rotational diffusion into the CSA principal axis system.

Since unrestricted rotational diffusion is not entirely realistic in describing internal motions in DNA, more sophisticated calculations of spectral densities, on the basis of internal jump models, have recently been advanced.[17,18] For the purposes of this paper, we have chosen to use the simpler motional model represented by eq 12-19 rather than the more sophisticated model we have already published[17] for two reasons. First, the relaxation data obtained for the three DNA forms (vide infra) indicates that the backbone internal motions are largely unaffected by the DNA form. Since we have already examined the nature of the internal motions of linear DNA in detail,[17] computer time could be more efficiently employed in calculations that require seconds to complete rather than hours. Second, despite the use of models that differ significantly in their detailed descriptions of the actual internal motions taking place in DNA, NMR relaxation experiments have produced a relatively unified picture of the magnitudes of the motional frequencies: at least one anisotropic internal rotation at a time scale of several nanoseconds for jumps (or subnanoseconds for diffusion) superimposed on a much slower isotropic reorientation with a correlation time of about 1-2 μs.

Properties of Supercoiled and Nicked-Circular DNA. In the B form of double-stranded linear DNA, each of the two strands follows the familiar helical curve in space. In supercoiled DNA, the two ends of the chain are covalently joined and the axis of the double helix itself describes a curved path in space, which, when projected onto a plane, will cross itself and form loops. The topological constraint imposed on the molecule by the fact that the two ends are covalently closed can be expressed in terms of the linking number L[19] such that

$$L = W + T \quad (20)$$

Here, W is the number of superhelical turns (the sign of W is determined by a configurational convention),[20] and T is the number of turns within the double helix itself; i.e., in linear DNA, normally $T = N/10$, where N is the number of base pairs. (T is positive for a right-handed helix.) L is invariant and can only be changed when one of the strands is nicked.

When a single-strand scission is introduced into supercoiled DNA, the nicked-circular form of DNA is obtained. The excess free energy of the supercoiled molecule, relative to the relaxed, nicked circle, can be estimated from the relation

$$\Delta G_s = CRTN\sigma^2 \quad (21)$$

where $\sigma = [W + (T - N/10)]/(N/10)$ is the superhelical density. There has been some uncertainty in the literature concerning the value of the constant C, with suggested values ranging from 5.4[21] to 10.[22-24]

(8) Abragam, A. "Principles of Nuclear Magnetism"; Clarendon Press: Oxford, England, 1961.
(9) Woessner, D. E. *J. Chem. Phys.* **1962**, *37*, 647-654.
(10) Hogan, M. E.; Jardetzky, O. *Proc. Natl. Acad. Sci. U.S.A.* **1979**, *76*, 6341-6345.
(11) Hogan, M. E.; Jardetzky, O. *Biochemistry* **1980**, *19*, 3460-3468.
(12) Woessner, D. E. *J. Chem. Phys.* **1962**, *36*, 1-4.
(13) Klevan, L.; Armitage, I. M.; Crothers, D. M. *Nucleic Acids Res.* **1979**, *6*, 1607-1616.
(14) Bolton, P. H.; James, T. L. *J. Phys. Chem.* **1979**, *83*, 3359-3366.
(15) Bolton, P. H.; James, T. L. *J. Am. Chem. Soc.* **1980**, *102*, 25-31.
(16) Hull, W. E.; Sykes, B. D. *J. Mol. Biol.* **1975**, *98*, 121-153.
(17) Keepers, J. W.; James, T. L. *J. Am. Chem. Soc.* **1982**, *104*, 929-939.
(18) Lipari, G.; Szabo, A. *Biochemistry* **1981**, *20*, 6250-6256.
(19) Fuller, F. B. *Proc. Natl. Acad. Sci. U.S.A.* **1971**, *68*, 815-819.
(20) Vinograd, J.; Lebowitz, J.; Watson, R. *J. Mol. Biol.* **1968**, *33*, 173-197.
(21) Hsieh, T. S.; Wang, J. C. *Biochemistry* **1975**, *14*, 527-535.

Figure 1. Results of a 1.5% agarose gel electrophoresis run of supercoiled (I), circular (II), and linear (III) pIns36. The gel was stained in an ethidium bromide solution and photographed under ultraviolet light.

The excess free energy ΔG_s that is trapped in the molecule may contain contributions from torsional or bending stresses as well as from an entropy term. As pointed out by Bauer and Vinograd,[22] this energy should be available to do work in processes aimed at reducing σ. The possible contribution of this excess energy to the breakage of hydrogen bonds and base-pair opening has already been considered,[6] but other processes such as reversible local bending and winding or unwinding motions could also be affected by ΔG_s. (Note that through the conservation condition of eq 20, bending and twisting motions are essentially coupled in superhelical DNA.)

So far we considered the internal free energy of supercoiled vs. nicked-circular DNA. The latter form is relieved from any torsional stresses but can be considered to occupy a higher configurational free energy level than the linear form of the same DNA, mainly due to the loss in configurational entropy involved in the ring closure. The free energy difference between the linear and circular polymer can be estimated from the cyclization probability $Q(\mathbf{0})$ of the linear form at thermal equilibrium. Such probabilities, as a function of chain length, were calculated by Olson[25] on the basis of realistic consideration of the double-helical stiffness and internal flexibility. For a 7-kilobase chain, the probability of ring closure is about 3.6×10^{-12}, leading to a free energy difference (at 298 K) of 15.6 kcal/mol.

Experimental Section

Plasmid pIns36 (7.2 kilobase) was derived from plasmid pBR322.[26] A 2.8-kilobase human DNA fragment was subcloned into the *Hin*dIII site of pBR322. The resulting plasmid has been designated as pIns36.

pIns36 was grown and amplified in *E. coli* HB101. The bacteria were lysed by treatment with lysozyme and Triton.[27] Plasmid DNA was separated from the bacterial DNA by low-speed (13 000 rpm) centrifugation. Plasmid DNA was extracted with phenol, and the closed-circular DNA (pIns36-I) was isolated from an ethidium bromide–CsCl bouyant density gradient.[28]

Closed-circular pIns36-I was converted into nicked-circular DNA (pIns36-II) by overnight incubation at 65 °C. Linear pIns36-III was obtained by exhaustive digestion of the DNA with restriction endonuclease *Eco*R1.[29]

(22) Bauer, W.; Vinograd, J. *J. Mol. Biol.* **1970**, *47*, 419–435.
(23) Depwe, R. E.; Wang, J. C. *Proc. Natl. Acad. Sci. U.S.A.* **1975**, *72*, 4275–4279.
(24) Pulleyblank, D. E.; Shure, M.; Teng, D.; Vinograd, J.; Vosberg, H. P. *Proc. Natl. Acad. Sci. U.S.A.* **1975**, *72*, 4280–4284.
(25) Olson, W. K. In "Nucleic Acid Geometry and Dynamics"; Sarma, R. H., Ed.; Pergamon Press: New York; 1980; pp 383–397.
(26) Bolivar, F.; Rodriguez, R. L.; Green, P. J. Betlach, M. C.; Heyneker, H. L.; Boyer, H. W.; Crosa, J. H.; Falkow, S. *Gene* **1977**, *2*, 95–113.
(27) Meagher, R. B.; Tait, R. C.; Betlach, M. C.; Boyer, H. W. *Cell* **1977**, *10*, 521–536.
(28) Radloff, R.; Bauer, W.; Vinograd, J. *Proc. Natl. Acad. Sci. U.S.A.* **1967**, *57*, 1514–1521.
(29) Yoshimori, R. N. Ph.D. Thesis, UCSF, 1971.

Table I. Experimental ^{31}P Relaxation Times and NOE's at 40.5 MHz, 25 °C, for pIns36 DNA in 0.1 M NaCl, 10 mM Na Cacodylate pH 7.0[a]

	T_1, s	T_2, s	NOE
linear	2.4 ± 0.2	0.019 ± 0.003	1.3 ± 0.1
circular	2.5 ± 0.2	0.25 ± 0.07	1.4 ± 0.15
supercoiled	1.64 ± 0.15	1.17 ± 0.10	1.45 ± 0.18

[a] Most of the values listed in this table represent averages of two or three measurements on each of two separate preparations of pIns36. Experiments were carried out on different days, and the uncertainties reflect both variations in reproducibility and error margins of the individual results.

All DNA samples in this study were routinely analyzed by agarose gel (1.5% cross-linked) electrophoresis. The results of such a gel are shown in Figure 1. Densitometer tracings of the electrophoresis results revealed that the pIns36-I form contained about 15% contamination by nicked circles, and the nicked-circular DNA contained about 15% of the linear form. The pIns-III sample showed no detectable signs of DNA other than the linear form.

All NMR samples were prepared by dialysis against a buffer containing 0.1 M NaCl, 10 mM cacodylic acid, and 2 mM EDTA at pH 7.0; 10% (v/v) of D_2O was added for a field-frequency lock. The samples contained DNA at final concentrations of 1.5–3 mM in base pairs.

NMR experiments were carried out on a Varian XL-100 spectrometer, interfaced to a Nicolet 1080 computer, operating at 40.5 MHz for ^{31}P with the 12-mm multinuclear MONA probe. Temperature was maintained at 25 ± 0.5 °C.

NOE values were determined by comparing the signal intensities between spectra obtained with the proton decoupler on continuously and spectra with the decoupler on during acquisition only. Longitudinal (T_1) and transverse (T_2) relaxation times were measured by the inversion–recovery (180°–τ–90°–τ–ACQ) and the Hahn spin–echo (90°–τ–180°–τ–ACQ) techniques, respectively, and the relaxation times calculated by fitting the intensities of the Fourier-transformed signals with standard programs in the Nicolet software (three-parameter T1IR and T2CP). The validity of the T_2 measurements on our instrument are discussed in a separate publication.[30]

The superhelical density (σ) of pIns36-I was determined by the Dye/θ method,[3] yielding a value of −0.11 ± 0.025 when corrected to the conditions of 25 °C and 0.1 M NaCl.[3] Since the largest negative σ values for most DNA's examined in the literature are about −0.09, we tend to believe that our true result is at the upper boundary of our uncertainty range. In any case, pIns36 does have a large negative superhelical density compared with the values of other DNA's isolated intact from natural environments, which are in the range of −0.03 to −0.09.

Results and Discussion

The ^{31}P NMR resonance of pIns36 consists of a signal centered at about 4.00 ± 0.05 ppm upfield from external trimethyl phosphate. The apparent widths at half-intensity (at 25 °C and under conditions of proton decoupling) were about 25 Hz for the supercoiled and circular DNA and broader (about 45 Hz) for the linear DNA. The breadth of these signals is believed to result mainly from chemical shift dispersions of the ^{31}P nuclei in the polymer. No significant change in the average chemical shift was detected between the three forms of the DNA. A comparison of the experimental signal-to-noise ratios did not reveal any significant loss in signal intensity for any of the three forms compared to the others. We determined, by comparison to the signal obtained from a standard phosphate sample, that these intensities represent the majority (>90%) of the total phosphorus present in the DNA samples.

Table I lists the results of the ^{31}P relaxation experiments. The relaxation times were measured in the presence of broad-band, square-wave-modulated proton decoupling. In the absence of proton decoupling, the apparent T_2 values for both the circular and supercoiled forms decreased considerably (to about 0.04 s), a fact that apparently reflects scalar relaxation by the 5′ protons.[30] (No T_2 measurements in the absence of proton decoupling were attempted for the linear DNA.) Both the relatively low signal-to-noise ratio in the individual spectra and the limited number of delay-time values in each experiment (between 6 and 9) pre-

(30) Bendel, P.; James, T. L. *J. Magn. Reson.* **1982**, *48*, 76–85.

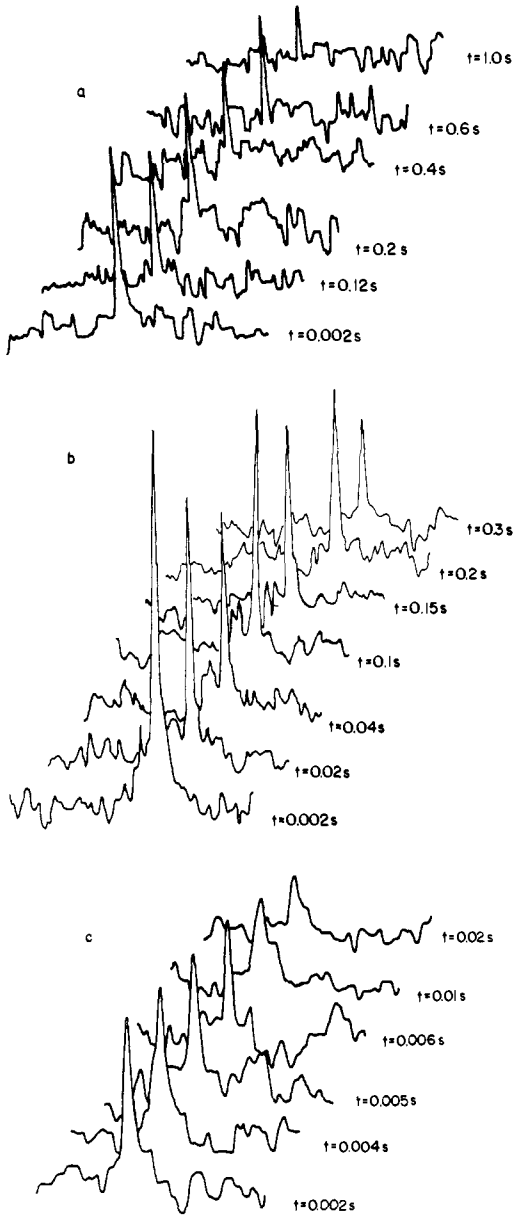

Figure 2. Results of some of the Hahn spin–echo experiments for pIns36 DNA, at 25 °C in 0.1 M NaCl, 10 mM cacodylic acid, and 2 mM EDTA, pH 7. Shown are ^{31}P Fourier-transformed spin echoes, under continuous proton irradiation, SW = ±1000 Hz, 1024 real points, acquisition time 0.512 s. The times of the echo occurrence are indicated in the figure. (a) Supercoiled DNA, 800 scans (per spectrum), pulse repetition time (for signal averaging) 7.5 s, exponential line broadening = 20 Hz. (b) Nicked-circular DNA, 1600 scans, prt = 8 s, line broadening = 25 Hz. (c) Linear DNA, 1560 scans, prt 3.2 s, line broadening = 50 Hz.

cluded the possibility of unambiguously identifying multiple components in the relaxation curves. One should therefore consider the listed T_2 values as averages representing at least 80% of the total phosphorus nuclei in the samples. Figure 2 shows some representative results of T_2 experiments on pIns36.

We now turn to the question of simulating the experimental results with a model for the relaxation. First the interaction strengths for the dipolar and CSA mechanisms have to be evaluated. The chemical shift anisotropy and asymmetry parameters can be obtained from the solid-state powder pattern of the ^{31}P resonance. Values from 99 ppm[33] to 109 ppm[31,32] have been reported for δ_z, whereas η is about −0.6. The dipolar relaxation is primarily due to intramolecular ^{31}P–^{1}H interactions, with negligible contributions from the solvent.[14,15] It is commonly accepted to use the B-DNA structure as representing the DNA conformation in solution, although recent evidence indicates that this may not be entirely true.[34-36] We have chosen to adopt a conformation resulting from an energy minimization procedure on the structure of a dodecamer, resulting in the internuclear phosphorus–hydrogen distances listed in Table IIA. These are very similar to the distances obtained from the coordinates of the fiber B-DNA structure,[37] with the most notable deviation being in a shortened effective P–H3′ distance, which is the result of allowing the sugar ring to repucker between the conformations characteristic of the B-DNA and A-DNA structures, as proposed by Keepers and James.[17] A schematic representation of the relevant molecular residue is depicted in Figure 3. We have not included the P–H4′, P–H2′, and P–H1′ interactions in our calculations since the distances between the phosphorus and these protons are considerably longer and their combined contribution is estimated to amount to less than 15% of the total dipolar relaxation or to 4%–10% of the total relaxation rates.

In agreement with previous reported observations, the experimental relaxation results for linear DNA cannot be simulated by using a single isotropic correlation time. This is also true for the data from the circular DNA. For supercoiled DNA, however, a single correlation time of 1.27 ns yields reasonable agreement with the experimental results (see Table IIIB).

Table II. Structural Parameters Used in the Calculations of Dipole–Dipole and CSA Relaxation Rates for ^{31}P in DNA

A. Dipole–Dipole		
internuclear vector	length, Å	angle, deg
P–H5′	2.70	119[a]
P–H5′	3.09	125[a]
P–H3′	2.88[c]	154[b]

B. Chemical Shift Anisotropy			
δ_z	η	β[d]	γ[d]
105 ppm	−0.60	90°	141°

[a] The angle is between the internuclear vector and the C4′–C5′ bond. [b] The angle is between the internuclear vector and the C3′–O3′ bond. [c] This is an $1/\langle r^6 \rangle$ average between the two jump states of sugar repuckering. [d] The Euler angles for rotating the CSA tensor into a molecular frame with the P–O3′ bond as the z axis.

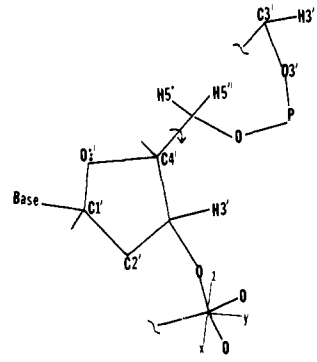

Figure 3. Schematic illustration of a nucleotide segment depicting the protons predominant in the dipole–dipole relaxation of the ^{31}P nucleus and the principal axis system of the phosphorus chemical shift tensor.

(31) Terao, T.; Matsui, S.; Akasaka, K. *J. Am. Chem. Soc.* **1977**, *99*, 6136–6138.
(32) Opella, S. J.; Wise, W. B.; DiVerdi, J. A. *Biochemistry* **1981**, *20*, 284–290.
(33) Shindo, H. *Biopolymers* **1980**, *19*, 509–522.
(34) Cohen, J. S.; Wooten, J. B.; Chaterjee, C. L. *Biochemistry* **1981**, *20*, 3049–3055.
(35) Mitra, C. K.; Sarma, M. H.; Sarma, R. H. *J. Am. Chem. Soc.* **1981**, *103*, 6727–6737.
(36) Mandelkern, M.; Dattagupta, M.; Crothers, D. M. *Proc. Natl. Acad. Sci. U.S.A.* **1981**, *78*, 4294–4298.
(37) Arnott, S.; Wilkins, M. H. F.; Hamiltin, L. D.; Langridge, R. *J. Mol. Biol.* **1965**, *11*, 391–402.

Table III. Calculated ^{31}P NMR Relaxation Times and NOE's at 40.5 MHz from Combined Dipole–Dipole and CSA Relaxation

A. Using the Two-Correlation-Time Model with Overall Isotropic Motion (τ_0) and Free Internal Diffusion (τ_i)

	τ_0, ns	τ_i, ns	T_1, s	T_2, s	NOE
linear[a]	860	0.36	2.28	0.018	1.40
circular[b]	56	0.25	2.53	0.25	1.52
supercoiled[c]	5.25	0.30	1.77	1.17	1.39

B. Using a Single Correlation Time for Isotropic Rotation

	τ_c, ns	T_1, s	T_2, s	NOE
supercoiled	1.27	1.48	1.27	1.44

[a] The uncertainty range in the experimental T_2 values can be accommodated by τ_0 values from 720 to 980 ns. While the possible range of T_1 values allows for τ_i values from 0.27 to 0.38 ns, the NOE would be outside the experimental error range for τ_i values shorter than 0.36 ns. [b] The uncertainty in the experimental results allows τ_0 values from 44 to 80 ns and τ_i values from 0.23 to 0.32 ns. [c] This is the longest τ_0 (and shortest τ_i) value compatible with the model and the experimental data. The range of experimental results can be fit by different combinations of correlations times down to $\tau_0 = 3.45$ ns and up to $\tau_i = 0.45$ ns.

Calculations using the two-correlation-time Woessner model (eq 10–19) and parameters listed in Table II lead to the results in Table IIIA. Our model assumes an isotropic reorientation of the bonds located in the backbone of the DNA molecule (C4′–C5′, C3′–O3′, and P–O3′) upon which much faster internal motions are superimposed. The time scale on which these internal motions occur is in agreement with previously published results. We would like to point out that the capability of the model to fit the experimental data is not, by itself, proof that the internal motion actually proceeds by unrestricted rotational diffusion as assumed in the model. On the other hand, it has been demonstrated[17] that even though the free internal diffusion model might not faithfully describe the motion occurring in the molecule, it will fit the experimental data for linear DNA with correlation times (both overall and internal) that are very similar to those needed in fitting the data by much more complicated and computer-time consuming calculations on the basis of more realistic internal-jump models.[17] On the basis of these observations, it seems that the frequencies of internal pseudorotation or jumps do not differ significantly between the three forms of DNA observed in this study and are in general agreement with the internal correlation times of motions around the backbone derived from previous studies.[13-15]

The most significant observation in our present work is the large difference in the spin–spin relaxation times between the supercoiled, circular, and linear forms of the DNA we investigated. These differences in relaxation rates could be caused either by differences in the interaction strengths or the isotropic correlation times (τ_0) or a combination of both. Considering the first possibility, it is very unlikely that either the chemical shift anisotropy or the average phosphorus–hydrogen distances could be different enough in supercoiled (compared to linear DNA) to account for a 60-fold increase in T_2. (This would require δ_z to be reduced to about 14 ppm and the P–H distances to be increased to 5.5 Å.) Another possibility would be changes in the geometric coefficients (eq 11–13 and 17–19). Such structural changes would have been reflected as well in altered T_1 values, however. We cannot, however, rule out completely the possibility that slight conformational changes do cause some reduction of the coefficients A and/or C_0 in supercoiled DNA. The large difference in T_2 would still have to be explained by a change in τ_0; albeit not as big a change as one would obtain by assuming that the interaction strengths are the same for all three forms of the DNA.

T_2 measurements on linear fragments of calf thymus DNA (up to a length of ~600 base pairs) have been previously reported by Hogan and Jardetzky.[10,11] They report values from 32 ms for the 140 base pair fragment down to 12 ms for the 600 base pair fragments, so that our results for linear pIns36 conform to these findings. Our calculated τ_0 value of 0.86 μs for the 7200 base pair linear pIns36 is also consistent with the value of 1 μs deduced by Bolton and James[14,15] from off-resonance $T_{1\rho}$ measurements on ca. 700 base pair long fragments of calf thymus DNA.

If the structural parameters (as listed in Table II) do not change significantly upon conversion of the DNA into a different topoisomeric form, then the changes in T_2 imply large changes in τ_0, the correlation time for isotropic reorientation. If one takes into account experimental uncertainties, the simulations indicate a reorientation rate that is about 140–280 times faster in supercoiled than in linear DNA, and 9–20 times faster in circular than in linear DNA.

Before exploring possible reasons for these observations, one must try to understand the motion characterized by the isotropic or "overall" correlation time τ_0. As already mentioned, the overall motion of very short DNA fragments can be described by end-over-end tumbling and rotation about the long axis of a rigid rod, and the correlation times predicted by fundamental hydrodynamic equations seem to fit the results of NMR relaxation experiments on such systems.[38] Longer DNA chains (≳200 base pairs), however, are usually modeled as "wormlike chains"[39] that, although more flexible than rigid rods, possess an internal stiffness (characterized by a persistence length a_0) making them less flexible than a random, Gaussian coil. In this case, it is much more difficult to quantitatively characterize the overall motion of the molecule. As a first approximation, the hydrodynamic behavior of the molecule could be treated as a solid sphere with a radius of gyration R_g. With the use of Zimm's normal coordinate theory,[39,41] the relaxation time for the first normal mode, which corresponds to a correlation time for the overall rotation, is given by

$$\tau_R = \frac{1.4\pi\eta_0 R_g^3}{kT} \tag{22}$$

Assuming R_g to be about 200 nm (Voordouw et al.[40] reported 186 nm for linear *Col*E$_1$ plasmid DNA, which is only slightly shorter than pIns36) and taking the bulk viscosity η_0 as 0.01 P, we arrive at τ_R = 8.6 ms, which is clearly much too slow to be responsible for the isotropic motion detected in our NMR experiments. Moreover, eq 22 roughly predicts a three-halves power dependence of τ_R (and therefore also $1/T_2$) on the total polymer length, whereas the results of Hogan and Jardetzky[10,11] on 300–600 base pair fragments, Bolton and James[14,15] measurements on ~700 base pair DNA, and our present findings on much longer chains of 7.2-kilobase length, indicate that there is little or no dependence of the isotropic correlation time responsible for T_2 on chain length for linear DNA longer than about one persistence length.

It is also possible that the τ_0 value can be identified with rotation about the helix axis for linear DNA. The correlation time for rotation about the long axis of a rod of length $2L$ and radius b in a medium of viscosity η can be calculated from the Lamb equation:[42]

$$\tau_{\parallel} = \frac{4\tau\eta b^2 L}{3kT} \tag{23}$$

According to eq 23, the correlation time would be linearly dependent on chain length if this potential rotation about the helix axis governed T_2. As noted above, however, T_2 is effectively unchanged as DNA length varies from 300 to 7200 base pairs.

These observations, namely that the hydrodynamic predictions for the overall reorientation of linear DNA chains fail to predict both the absolute value of the isotropic correlation times observed in the NMR experiments and their dependence on chain length, have led to the suggestion[14,15] that the isotropic reorientation responsible for these relatively short correlation times consists of

(38) Hart, P. A.; Anderson, C. F.; Hillen, W.; Wells, R. D. In "Proceedings of the 2nd SUNYA Conversation in the Discipline Biomolecular Stereodynamics"; Sarma, R. H., Ed.; Adenine Press: New York, 1981; Vol. 1.

(39) Bloomfield, V. A.; Crothers, D. M.; Tinocco, I., Jr. "Physical Chemistry of Nucleic Acids"; Harper and Row: New York, 1974.

(40) Voordouw, G.; Kam, Z.; Borochov, N.; Eisenberg, H. *Biophys. Chem.* **1978**, *8*, 171–189.

(41) Zimm, B. H. *J. Chem. Phys.* **1956**, *24*, 269–278.

(42) Barkley, M.; Zimm, B. H. *J. Chem. Phys.* **1979**, *70*, 2991–3007.

a segmental bending motion of the DNA backbone. As discussed previously,[14,15] bending motions can be isotropic.

Barkley and Zimm[42] derived a theoretical model for bending motions of linear DNA. From their treatment (eq VI.3 in ref 42), bending modes with relaxation times of the order of 1 μs should have wavelengths of about 400 base pairs. While higher order bending modes with shorter wavelengths and faster relaxation times may exist, they are apparently not efficient enough in reorienting the vectors along the DNA backbone.

Turning back to our original question of the decrease in τ_0 for supercoiled and circular DNA, we note that simple hydrodynamic considerations (as expressed in eq 22) do predict this trend, at least qualitatively. Due to their configurational restrictions, circular and (even more so) supercoiled DNA have smaller average dimensions than linear DNA of the same molecular weight. Quantitatively, however, eq 22 fails to account for the observed ratios in correlation times between the three forms. Referring again to the data on *Col*E$_1$,[40] we see that eq 22 predicts τ_R to be three times faster in circular and six times faster in the supercoiled DNA compared to the linear form. These ratios fall short of experimental results by an order of magnitude in the case of supercoiled DNA.

If segmental bending motions are primarily responsible for the observed T_2 values, there could be two reasons for our observation of higher flexibility in the circular and supercoiled forms. First, the relaxation time for each bending mode could be intrinsically shorter for these molecules. A quantitative evaluation of this possibility can only be given by a careful theoretical derivation such as the study by Barkley and Zimm[42] applied to circular and supercoiled DNA. The second possibility is that the higher order modes with shorter correlation times are more prominently represented in the spectrum of bending motions of the molecule or that these bending motions with higher frequency could be of larger amplitudes so that they become much more effective in producing NMR relaxation. We shall now try to elaborate upon why this second possibility seems plausible to us.

The basic distinction of both the nicked-circular and supercoiled forms is that they are closed chains, and one might therefore anticipate encountering higher order bending waves, much like overtones occurring in a string that is tied at both ends. Another way of putting it is that bending energy, which is dissipated to the solvent by the open ends of the linear form, continues to propagate along the chain in the closed forms.

A larger population of high-frequency bending modes (or larger amplitudes produced by these modes) can occur if the molecule contains energy that does work in these motions. As a crude approximation, one can describe the bending motions as first-order rate processes and convert the observed ratios in correlation times (or "rate constants") into energy differences between the ground states. This would imply that the circular and supercoilel DNA's (or appropriate segments within the molecules) are about 1.5 and 3 kcal/mol closer, respectively, to the "transition state" than linear DNA. As already mentioned, superhelical DNA contains a huge amount of excess free energy compared to the linear form, in our case about 200–300 kcal/mol. (It is important to remember that this free energy results only from conformational stresses and not from covalent or hydrogen bonds, since our comparison is to a linear molecule without "sticky" ends.) If all this energy was channeled into the local, reversible bending deformations and uniformly distributed over the molecule, then a segment of about 60–110 base pairs would contain the required 3 kcal/mol to account for the observed difference in bending frequencies. For circular DNA, which we estimated to contain an excess of 15 kcal/mol over the linear form, 1.5 kcal/mol would be contained in a $\sim$700 base pair segment.

We mentioned before that, due to conservation of the linking number, twisting and bending motions should essentially be coupled in supercoiled DNA. Torsional motions occur on a nanosecond time scale[42] but do not produce, by themselves, enough reorientation to cause efficient NMR relaxation.[17] In supercoiled DNA, however, they could act as a "driving force" that causes high-frequency bending motions.

One might wonder whether the results for the circular DNA were not influenced by the fact that the circles in our sample apparently contained a number of single-stranded nicks (see Experimental Section). However, even a large number of single-stranded nicks does not significantly alter the intrinsic stiffness of the double-helical chain.[39] Moreover, the linear form we looked at was derived from the circular sample directly, so that it should contain about the same amount of single-stranded nicks.

Finally, we cannot rule out the possibility that other interesting properties of supercoiled DNA are at least partially responsible for our NMR relaxation results. We specifically refer to the already mentioned sharp increase in the occurrence probabilities of single-standed regions[6] and cruciform structures,[6,43] particularly for molecules with a high (negative) superhelical density.

Conclusions

A comparison of phosphorus-31 relaxation parameters (T_1, T_2, and NOE) between the three topoisomeric forms of pIns36, a 7.2-kilobase intact plasmid DNA in solution, revealed little or no differences in the NOE's and the spin–lattice relaxation times, while the spin–spin relaxation times increased by a factor of 8–20 in circular DNA (compared to the linear form) and by an additional factor of 3–7 in the supercoiled form.

On the basis of this and earlier work,[10–13,17,33] it is clear that the ^{31}P, T_1, and NOE values of native DNA are governed by a fast internal motion on a nanosecond or subnanosecond time scale. From further probing of the spectral densities of molecular motion at lower frequencies by T_2 or $T_{1\rho}^{off}$ measurements,[10,11,14,15] it became further evident that this fast internal motion could not be isotropic and that isotropic reorientation is achieved by a slower motional component with a correlation time of about 1 μs.

The exact nature of the motion that causes isotropic reorientation on a microsecond time scale is not clear. Both the magnitude of this correlation time and the absence of any molecular dependence contradict its identification with overall tumbling of the whole molecule. It was thus proposed that segmental bending motions of the chain are primarily responsible for the isotropic reorientation.

Our present results for linear DNA agree with previous observations on much shorter DNA. The similarity in the T_1 and NOE values for linear, circular, and supercoiled DNA indicate that the internal motions in these three forms occur on the same time scale. The slower motion correlation times, mainly reflected in the T_2 relaxation times, are much faster in circular and faster yet in the supercoiled forms compared to linear DNA. While this trend is expected for overall tumbling of the whole molecule, the magnitude of the change cannot be explained by simple hydrodynamic considerations.

We interpret the faster isotropic correlation times encountered in circular and supercoiled DNA as reflecting an increased proportion of faster bending motions. These phenomena can be rationalized by taking into account some of the characteristic physical properties of the closed forms. Ring enclosure (for circular and supercoiled) and conservation of a topological linking number (for supercoiled) trap an additional substantial amount of free energy within the molecule, part of which apparently becomes available for enhancing higher frequency bending modes.

It should be of interest to further scrutinize these ideas both theoretically and experimentally. Fluorescence depolarization experiments have not been reported, as far as we know, for supercoiled DNA, although this and other methods of dynamic observation are more sensitive to torsional than to bending motions.

Note Added in Proof. After this manuscript was submitted, two publications probing the internal dynamics of supercoiled DNA came to our attention. In a fluorescence depolarization study (Millar, D. P.; Robbins, R. J.; Zewail, A. M. *J. Chem. Phys.* **1982**, *76*, 2080–2094), it was found that pBR322 had a 30% higher

(43) Panayotatos, N.; Wells, R. D. *Nature (London)* **1981**, *289*, 466–470.

(44) The conventional definition for the correlation time is $1/D_i$ for jump models and $1/6D_i$ for diffusion models, where D_i is the internal motion rotational diffusion coefficient.

torsional rigidity than linear DNA. It is not clear whether a direct relevance to the NMR experiment exists because the fluorescence depolarization results are quite insensitive to bending motions and also because the intercalated ethidium bromide might significantly alter the dynamic properties of the supercoiled DNA compared to its natural form. In another study, conducted by the perturbed $\gamma-\gamma$ angular correlation (PAC) method (Martin, P. W.; El-Kuteb, S.; Kuhnlein, U. *J. Chem. Phys.* **1982**, *76*, 3819-3822) on supercoiled PM2 DNA, and apparent isotropic correlation time of 8.2 ± 0.6 ns was measured, compared to 62 (+12/−10 ns) for presumably much more flexible single-stranded DNA (Kolfas, C. A.; Sideris, E. G.; El-Kuteb, S.; Martin, P. W.; Kuhnlein, U. *Chem. Phys. Lett.* **1980**, *73*, 311-314). Although the agreement with the NMR results, both in the trend and the absolute value of τ_c is intriguing, it is not clear how much of the correlation time observed by PAC is due to internal mobility of the ^{111}In probe at the binding site.

In any case, it appears that some of the unique properties of superhelical DNA are accessible to NMR experiments and that these might help to elucidate the importance of this DNA form in biological processes.

Acknowledgment. Financial support for this research was provided by research grants GM25018 and CA27343 from the National Institutes of Health. T.L.J. also wishes to acknowledge receipt of a Research Career Development Award (AM00291) from the National Institutes of Health.

Isolation and Characterization of Pyrimidine–Psoralen–Pyrimidine Photodiadducts from DNA

David Kanne, Kenneth Straub, John E. Hearst,* and Henry Rapoport

Contribution from the Department of Chemistry and Lawrence Berkeley Laboratory, University of California, Berkeley, California 94720. *Received February 16, 1982*

Abstract: We report the isolation and characterization for the first time of pyrimidine–psoralen–pyrimidine photodiadducts from DNA. For each of the four psoralens studied, a single pair of diastereomeric thymidine–psoralen–thymidine photodiadducts, each with cis-syn stereochemistry, was found to account for >90% of the diadducts formed. In addition, we have carried out pulse–chase experiments that establish that these photo cross-links are formed by cycloaddition of a second thymidine residue to the 3,4 double bond (pyrone side) of an initially formed 4′,5′ (furan-side) psoralen–thymidine photomonoadduct.

The reaction between the photosensitizing drugs known as psoralens (structures **1**–**4**) and nucleic acids has been the subject of intense study. This interest stems in part from the successful

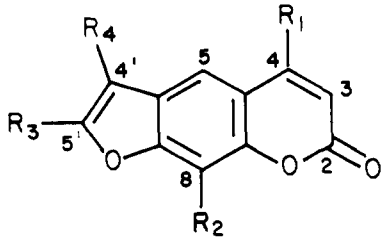

1, $R_1 = R_2 = R_3 = R_4 = H$
2, $R_1 = R_2 = R_3 = CH_3$; $R_4 = H$
3, $R_1 = R_3 = R_4 = H$; $R_2 = OCH_3$
4, $R_1 = R_2 = R_3 = H$; CH_3; $R_4 = CH_2OH$

application of psoralens in combination with 320–380-nm light as an effective treatment for vitiligo and psoriasis (PUVA therapy)[1,2] and because psoralens have become a useful tool for studying the structure and dynamics of nucleic acids. These studies include the use of the psoralen–nucleic acid reaction as a probe of chromatin structure,[3] the mapping of DNA–protein interactions,[4] and the "freezing" of DNA and RNA secondary and tertiary structures.[5,6] In addition, psoralens are under investigation as a potentially significant class of naturally occurring mutagens and carcinogens, and caution has been urged against the unrestricted use of psoralens in photochemotherapy.[7,8]

The event that is central to these different applications is the photochemical reaction that takes place between the psoralen and the nucleic acid. The photoaddition is a two-step reaction, where the initially formed products are psoralen–nucleoside monoadducts. Upon absorption of a second photon, properly positioned monoadducts can undergo further photoreaction with pyrimidine residues on the complementary nucleic acid chain, resulting in cross-linking of the two strands. The presence of covalent cross-links can be demonstrated by denaturation–renaturation kinetics[9] or by direct visualization of the cross-linked DNA by electron microscopy under totally denaturing conditions.[10,11] It is this ability to efficiently form interstrand cross-links that is the basis for the use of psoralen as a probe of nucleic acid structure.

While reports have appeared on the structural characterization of a number of psoralen–nucleoside monoadducts,[12,13] the diadduct(s) responsible for interstrand cross-linking has yet to be identified. In this study we report on the isolation and characterization of the principal nucleoside–psoralen–nucleoside diadducts formed in the photoreaction of four different psoralens with native, double-stranded DNA. Two of these, 4,5′,8-trimethylpsoralen (trioxsalen or TMP, **2**) and 8-methoxypsoralen (xanthotoxin or 8-MOP, **3**), are the most commonly used medicinal furocoumarins. The third psoralen, 4′-(hydroxymethyl)-4,5′,8-trimethylpsoralen (HMT, **4**), is a synthetic derivative with en-

(1) Scott, B. R.; Pathak, M. A.; Mohn, G. R. *Mutat. Res.* **1976**, *39*, 29.
(2) Parrish, J. A.; et al. *N. Engl. J. Med.* **1974**, *291*, 1207-1211.
(3) Wiesehahn, G. P.; Hyde, J. E.; Hearst, J. E. *Biochemistry* **1977**, *16*, 925-932.
(4) Hanson, C. V.; Shen, C.-K. J.; Hearst, J. E. *Science (Washington, D.C.)* **1976**, *193*, 62-64.
(5) Wollenzien, P. L.; Youvan, D. C.; Hearst, J. E. *Proc. Natl. Acad. Sci. U.S.A.* **1978**, *75*, 1642.
(6) Shen, C.-K. J.; Hearst, J. E. *Proc. Natl. Acad. Sci. U.S.A.* **1976**, *73*, 2649-2653.
(7) Stern, R. S.; Thibodeau, L. A.; Kleinerman, R. A.; Parrish, J. A.; Fitzpatrick, T. B. *N. Engl. J. Med.* **1979**, *300*, 809-813.
(8) Ashwood-Smith, M. J.; Poulton, G. A.; Barker, M.; Mildenberger, M. *Nature (London)* **1980**, *285*, 407-409.
(9) Cole, R. S. *Biochem. Biophys. Acta* **1970**, *217*, 30-39.
(10) Hanson, C. V.; Shen, C.-K. J.; Hearst, J. E. *Science (Washington, D.C.)* **1976**, *193*, 62-64.
(11) Cech, T. R.; Pardue, J. L. *Cell (Cambridge, MA)* **1977**, *11*, 631-640.
(12) Straub, K.; Kanne, D.; Hearst, J. E.; Rapoport, H. *J. Am. Chem. Soc.* **1981**, *103*, 2347-2355.
(13) Kanne, D.; Straub, K.; Rapoport, H.; Hearst, J. E. *Biochemistry* **1982**, *21*, 861-871.

0002-7863/82/1504-6754$01.25/0